AMERICAN SOCIETY FOR MICROBIOLOGY | Antimicrobial Agents and Chemotherapy®

PHARMACOLOGY

Development of Neutropenic Murine Models of Iron Overload and Depletion To Study the Efficacy of Siderophore-Antibiotic Conjugates

James M. Kidd,[a] Kamilia Abdelraouf,[a] David P. Nicolau[a]

[a]Center for Anti-Infective Research and Development, Hartford Hospital, Hartford, Connecticut, USA

ABSTRACT Siderophore-antibiotic conjugates have increased *in vitro* activity in low-iron environments where bacteria express siderophores and associated transporters. The host immune hypoferremic response reduces iron availability to bacteria; however, patients with iron overload or deficiency may have altered ability to restrict iron, which may affect the efficacy of siderophore-antibiotic conjugates. *In vivo* models of infection with iron overload and deficiency are needed to perform this assessment. The standard neutropenic murine thigh infection model was supplemented with iron-altering treatments: iron dextran at 100 mg/kg of body weight daily for 14 days to load iron or deferoxamine at 100 mg/kg daily plus a low-iron diet for up to 30 days to deplete iron. Human-simulated regimens of cefiderocol and meropenem were administered in both models to assess any impact of iron alteration on plasma pharmacokinetics. Median iron in overloaded mice was significantly higher than that of controls in plasma (1,657 versus 336 μg/dl; $P < 0.001$), liver (2,133 versus 11 μg/g; $P < 0.001$), and spleen (473 versus 144 μg/g; $P < 0.001$). At 30 days, depleted mice had significantly lower iron than controls in liver (2.4 versus 6.5 μg/g; $P < 0.001$) and spleen (72 versus 133 μg/g; $P = 0.029$) but not plasma (351 versus 324 μg/dl; $P = 0.95$). Cefiderocol and meropenem plasma concentrations were similar in iron overloaded and control mice but varied in iron-depleted mice. The iron-overloaded murine thigh infection model was established, and human-simulated regimens of cefiderocol and meropenem were validated therein. While deferoxamine successfully reduced liver and splenic iron, this depleting treatment altered the pharmacokinetics of both antimicrobials.

KEYWORDS animal models, conjugation, immune response, iron regulation, pharmacokinetics, siderophores

Siderophore-antibiotic conjugates, such as cefiderocol, exploit bacterial iron scavenging to achieve *in vivo* efficacy against a variety of Gram-negative bacteria, including multidrug-resistant strains (1). As part of the innate immune response to infection, extracellular iron concentrations are decreased by upregulation of hepcidin, a protein produced in the liver that is responsible for the hypoferremic response, starving bacteria of this essential nutrient (2, 3). In response, Gram-negative bacteria release endogenous siderophores to scavenge iron and increase the expression of membrane-bound ports for the iron-bound siderophores to reenter the cell (4). By hijacking this system, the uptake of siderophore-antibiotic conjugates is enhanced under *in vitro* conditions with low iron concentrations, leading to increased antibacterial activity, as has been observed in *Escherichia coli* (5) and *Pseudomonas aeruginosa* (6). Given the relationship between iron availability to the pathogen and MICs of siderophore-antibiotic conjugates, it is unknown how host iron overload or depletion affects the *in vivo* efficacy of these agents.

Citation Kidd JM, Abdelraouf K, Nicolau DP. 2020. Development of neutropenic murine models of iron overload and depletion to study the efficacy of siderophore-antibiotic conjugates. Antimicrob Agents Chemother 64:e01961-19. https://doi.org/10.1128/AAC.01961-19.

Address correspondence to David P. Nicolau, david.nicolau@hhchealth.org.

For a companion article on this topic, see https://doi.org/10.1128/AAC.01767-19.

Received 28 September 2019
Accepted 20 October 2019
Accepted manuscript posted online 28 October 2019
Published 20 December 2019

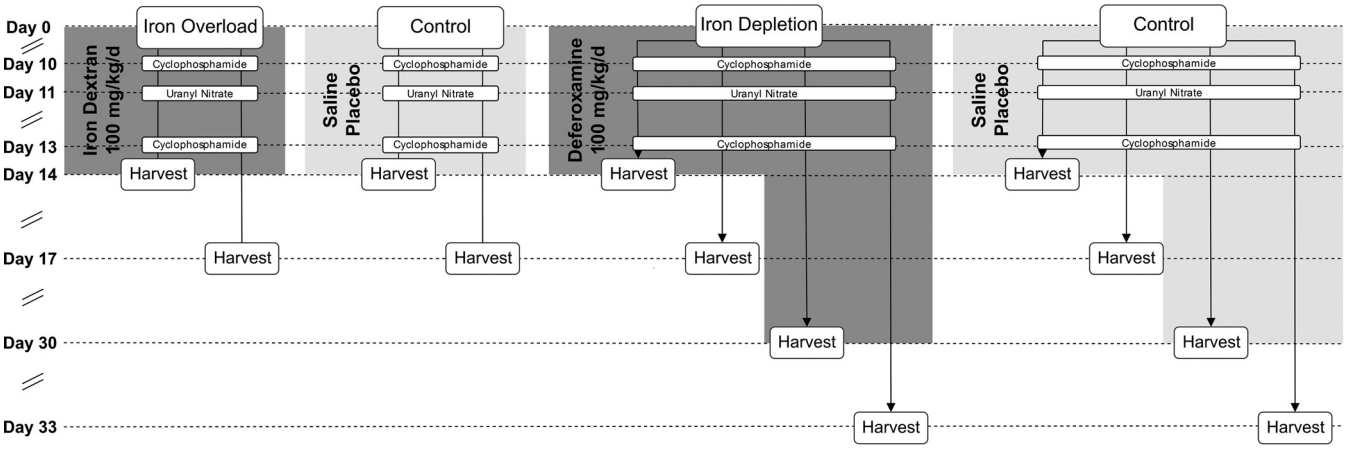

FIG 1 Study schematic for model development.

Alterations in iron status are common: patients with reduced or absent ability to produce hepcidin, such as those with hemochromatosis or chronic liver disease, can develop iron overload, placing them at greater risk for infection (7, 8). Iron overload is also seen in patients who are dependent on blood transfusions, such as those with thalassemia, sickle cell disease, or myelodysplastic syndromes (9). Iron deficiency is the most common nutritional deficiency worldwide. In developing countries, it most often results from insufficient dietary iron intake, while in developed countries failure to properly absorb iron is the major culprit, as in the case of gastrectomy, gastric bypass surgery, celiac disease, or *Helicobacter pylori* colonization (10, 11). A number of chronic diseases are associated with iron deficiency, including chronic heart failure, chronic kidney disease, and cancer (10). Furthermore, obesity has a negative effect on iron absorption through induction of hepcidin and is a risk factor for iron depletion. Given the incidence of iron status alteration, the *in vivo* efficacy of siderophore antibiotics in the setting of altered host iron statuses demands study, which requires a suitable, pragmatic model combining infection with altered iron status.

RESULTS

Iron overload and depletion models. Mice were given iron dextran to induce iron overload or deferoxamine and an iron-deficient diet to deplete iron, while same-age controls were dosed with saline on the same schedule. The impact of these treatments on total iron in plasma, liver, and spleen was compared; a schematic of the study design is presented in Fig. 1. At baseline, median [interquartile range (IQR)] iron content in all untreated 0-day samples (overload and depletion) was 574 (451 to 612) μg/dl in plasma, 11.6 (9.8 to 12.7) μg/g in liver, and 38.9 (33.0 to 47.2) μg/g in spleen. Compared to same-day control mice, mice treated with 14 days of iron dextran had significant ($P < 0.05$) increases in plasma (1,657 [943 to 2,402] μg/dl), spleen (473 [421 to 585] μg/g), and liver (2,133 [1,744 to 2,742] μg/g) (Fig. 2A). Deferoxamine treatment produced no statistically significant differences in iron content in any tissue with 14 days of treatment. However, 30 days of deferoxamine did significantly reduce iron content in liver (2.4 [2.3 to 2.9] μg/g) and spleen (72 [34 to 91] μg/g) compared with same-day controls (6.5 [5.7 to 7.7] μg/g and 133 [112 to 156] μg/g, respectively) (Fig. 2B), although plasma iron in deferoxamine-treated mice (351 [285 to 414] μg/dl) did not significantly differ from controls (324 [285 to 433] μg/dl). All significant differences at 14 days and 30 days were sustained for at least 3 days (i.e., at 17 days and 33 days, respectively) in the absence of iron dextran or deferoxamine treatment.

Pharmacokinetic studies. Pharmacokinetic studies were performed to assess effects of iron overloading or depleting treatments on human-simulated regimens of

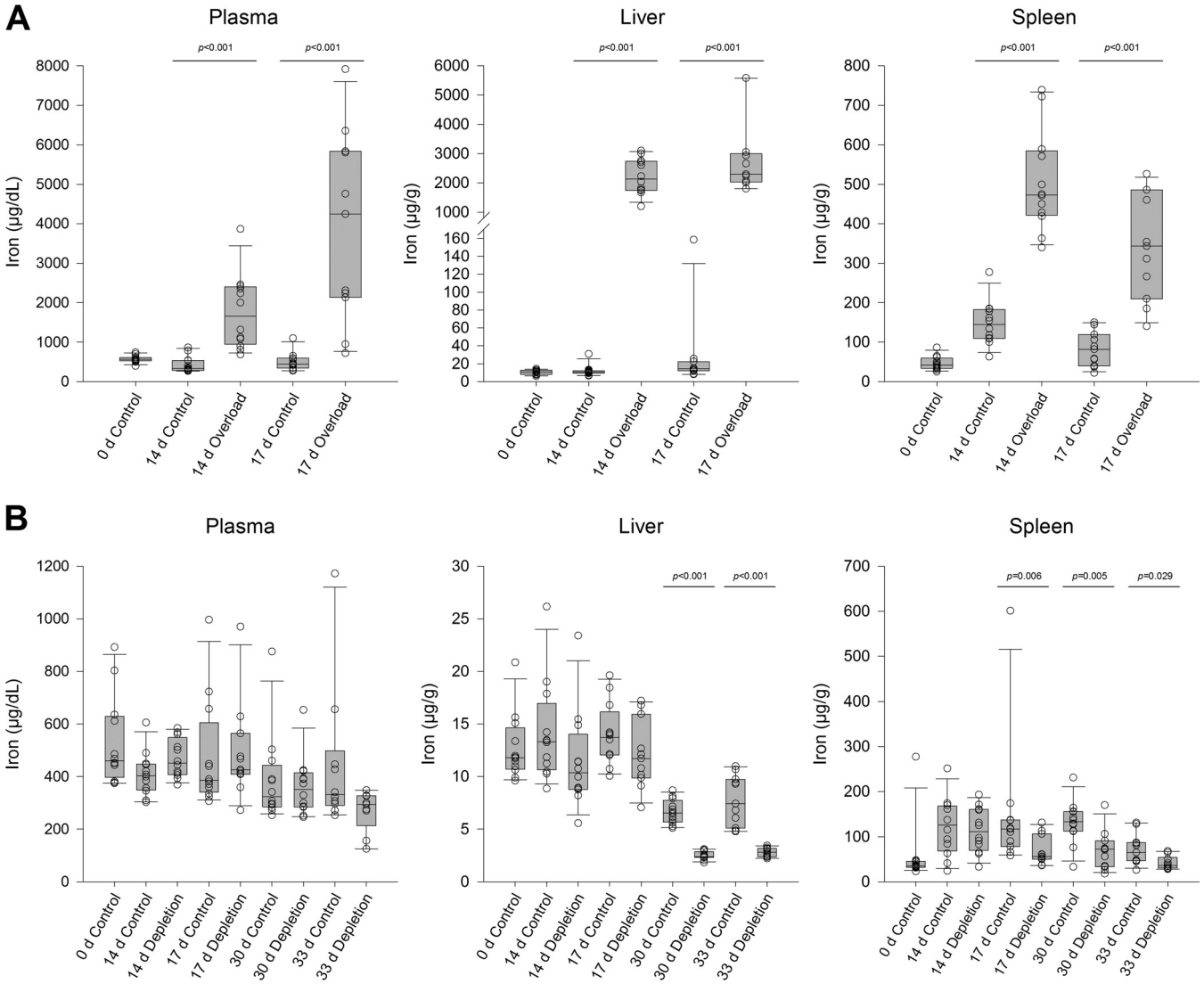

FIG 2 Measured iron concentrations (open circles) in murine plasma, liver, and spleen tissue for iron-overloaded mice (A) and iron-depleted mice (B). Horizontal lines within boxes represent median values, while box lower and upper borders represent 1st and 3rd quartiles. Whiskers represent 10th and 90th percentiles.

cefiderocol and meropenem. The pharmacokinetics of cefiderocol and meropenem were not altered by 14 days of treatment with iron dextran (Fig. 3). Mean weights were similar in iron-overloaded (24.3 ± 1.6 g) and control (26.4 ± 2.1 g) mice. For all 4 time points at which each human-simulated regimen was assessed, plasma concentrations of cefiderocol and meropenem were not significantly different between iron-overloaded and standard neutropenic murine thigh infection models, and both murine profiles were comparable to the human profile.

In the iron depletion model, cefiderocol concentrations were comparable to expected murine and human profiles, but same-age controls had significantly higher concentrations at 3 time points (Fig. 4). Mean weights were similar in iron-depleted (28.2 ± 2.3 g) and control (29.4 ± 2.8 g) mice. To assess the possibility of an interaction between the cefiderocol assay and any residual deferoxamine in the mice, an *ex vivo* interaction study was performed (Table 1). Known cefiderocol concentrations added to deferoxamine-treated mouse plasma were accurately measured, indicating that observed *in vivo* differences were not due to an interaction between deferoxamine and the cefiderocol assay. Meropenem concentrations were lower than expected in both iron-depleted and standard models.

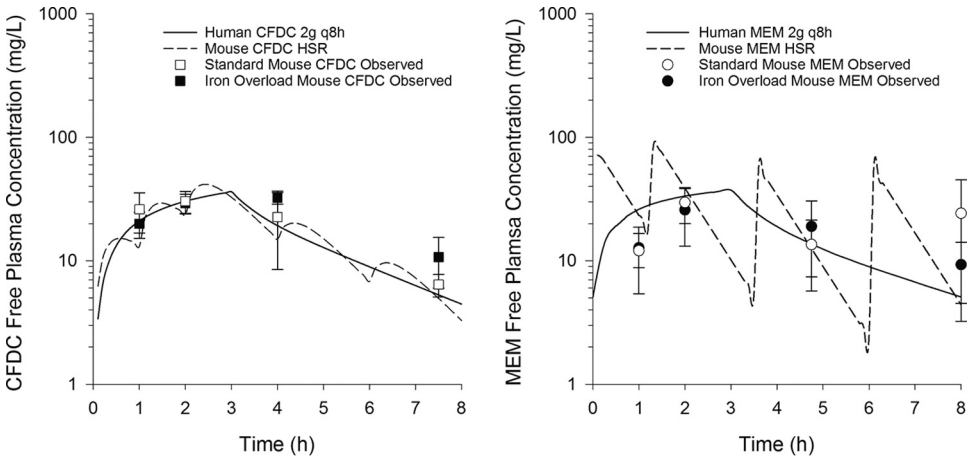

FIG 3 Pharmacokinetics of cefiderocol (CFDC) and meropenem (MEM) human-simulated regimens (HSR) in standard and iron overload murine thigh infection models. Data points are means, and error bars represent 95% confidence intervals.

DISCUSSION

Disorders of iron homeostasis frequently affect patients, and due to the interactions between iron status and infection (12), they warrant investigation as comorbidities in animal models of infection used to predict the efficacy of antibiotics, particularly siderophore-antibiotic conjugates. Several siderophore-antibiotic conjugates have been studied, most frequently β-lactams, but also quinolones and vancomycin (13). Siderophore-antibiotic conjugates are especially important to study in models of infection with altered iron statuses because of their iron-dependent Trojan horse mechanism of action, which has been shown to be more effective against Gram-negative bacteria under iron restrictive conditions (4). The models developed here provide an important translational setting to study efficacy of any such compounds before they are studied in patients with iron-related disorders.

The models of iron overload and depletion presented here were established in outbred mice with the induced neutropenia and renal dysfunction used in the standard thigh infection model. While knockout mouse models of hereditary hemochromatosis (14) and anemia of inflammation (15) recapitulate alterations in iron status, these models are less conducive to the translational study of bacterial infections, in part due

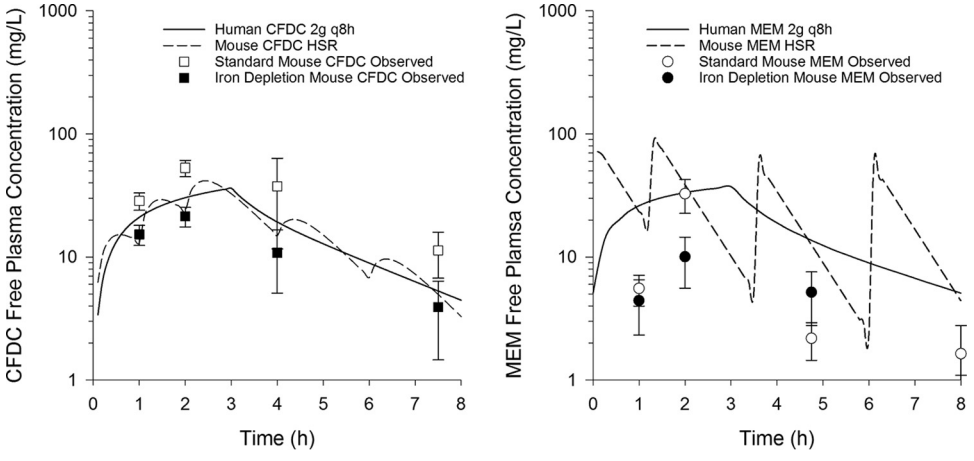

FIG 4 Pharmacokinetics of cefiderocol (CFDC) and meropenem (MEM) human-simulated regimens (HSR) in standard and iron depletion murine thigh infection models. Data points are means, and error bars represent 95% confidence intervals. The 8-h MEM free plasma concentration in the iron depletion model is not displayed because it was <1 (0.61 ± 0.48) mg/liter.

TABLE 1 Results of *ex vivo* interaction study between cefiderocol and plasma from deferoxamine-treated mice

Model	Cefiderocol concn (mg/liter)	Measured cefiderocol concn (mg/liter) by day after deferoxamine cessation		
		1	3	7
Standard	50	47.2 ± 4.0	49.7 ± 1.1	49.1 ± 1.5
Iron depletion	50	49.4 ± 1.5	49.3 ± 1.4	51.2 ± 4.1
Standard	5	4.9 ± 0.3	5.3 ± 0.1	5.2 ± 0.2
Iron depletion	5	5.1 ± 0.4	5.1 ± 0.6	5.4 ± 0.8

to the large number of animals necessary for such studies. For each individual bacterial strain studied in the neutropenic murine thigh infection model, a minimum of 3 to 6 animals are used per study group. A minimum of 3 groups, including a baseline 0-h control group, a 24-h control group, and a 24-h treatment group, are usually used; thus, studying a single therapy against a single strain requires 9 to 18 animals. At the scales on which these studies are typically performed, utilizing dozens of isolates and often comparing multiple treatments, obtaining sufficient numbers knockout mice could be time- and cost-prohibitive.

Deferoxamine treatment, coupled with a low-iron diet, was able to reduce hepatic iron and, to a lesser extent, splenic iron. Liver iron content in both control and iron depletion groups was lower than an estimate of liver iron content in iron-deficient patients (16); no such estimates of splenic iron content were found in the literature for comparison. Previous animal models of iron deficiency achieved with chelators have used a statistically significant decrease in tissue iron content as a marker of iron depletion (17, 18), as was achieved in the present study. In contrast to the iron reduction observed in liver and spleen, iron content was not reduced in plasma, possibly due to tight regulation of serum iron by transferrin; deferoxamine has also failed to reduce serum iron in rat and rabbit models (19, 20).

In the iron depletion model, the pharmacokinetic profile of a siderophore-antibiotic conjugate, cefiderocol, was altered compared with same-age controls. *Ex vivo* investigations showed that these alterations were not due to interactions between cefiderocol and residual deferoxamine that may have remained in the mice as a result of uranyl-nitrate-induced renal impairment, suggesting a physiological cause instead. For meropenem, a non-siderophore antibiotic, concentrations were also altered, and to a greater degree. These results have importance for future researchers wishing to study siderophore and non-siderophore β-lactams in the setting of iron depletion, as deferoxamine and/or the 30-day depletion period caused physiological changes in mice that affect plasma pharmacokinetics. Therefore, as a prerequisite to comparative efficacy studies, previously established antibiotic dosing regimens will require adjustment to match exposures between iron-depleted and standard murine thigh infection models.

Treatment with 14 days of iron dextran successfully produced supranormal iron concentrations in the liver, the primary organ of iron storage, which becomes saturated with iron in hereditary hemochromatosis (21), as well as the spleen, which receives iron from erythrocyte lysis associated with thalassemia and blood transfusions (22). The median iron concentration achieved in the liver in the iron overload model, 2,133 μg/g wet tissue, is within the range of liver iron levels seen in chronically iron-overloaded patients (16) and is greater than the threshold at which chelation therapy has been recommended for thalassemia (2,100 μg/g wet tissue, assuming 70% water content) (23, 24). As such, we have modeled specific tissue iron excesses observed with a variety of disease states associated with iron overload. Furthermore, the iron dextran treatment produced plasma iron concentrations well above the reported total iron binding capacity in mice (25), suggesting that much of the plasma iron was non-protein bound and, therefore, freely available to bacteria. Iron overload, particularly in the presence of non-protein-bound iron, theoretically poses a greater threat to siderophore-antibiotic conjugate efficacy than iron depletion, as free iron suppresses activity *in vitro* (6).

In contrast to the iron depletion model, pharmacokinetic profiles of cefiderocol and meropenem were unaltered in the iron overload model. Plasma concentrations of both drugs were comparable to those previously observed in the standard thigh infection model using these regimens (1, 26, 27), permitting a direct comparison of efficacy between iron-overloaded and standard murine thigh infection models.

Significant alterations in tissue iron content in both models were sustained for 3 days, permitting future 72-h *in vivo* efficacy studies in the setting of altered iron statuses. These studies are informative for siderophore-antibiotic conjugates given observations of adaptive resistance mediated by mutations in iron uptake systems (28, 29) and have been performed in the standard murine thigh infection model with cefiderocol (27).

In summary, pragmatic models of comorbid iron overload or depletion were developed on top of the standard neutropenic murine thigh infection model. Although the models do not replicate the typical human disease processes that lead to abnormal iron levels, most importantly, they produce a similar result. These models provide the opportunity to study the efficacy of siderophore-antibiotic conjugates under conditions that mimic clinical extremes of iron status. Such investigations will inform decisions about whether these antibiotics are safe and effective in patients with altered iron statuses.

MATERIALS AND METHODS

Pharmaceutical agents. Iron dextran (CAS 9004-66-4) solution and deferoxamine mesylate (CAS 138-14-7) powder were obtained from Millipore Sigma (St. Louis, MO) and stored at room temperature and −80°C, respectively. Cefiderocol 500-mg vials were obtained from Shionogi & Co., Ltd. (Osaka, Japan), and stored at −80°C. Meropenem 500-mg vials (Fresenius Kabi USA, Lake Zurich, IL) were obtained from Cardinal Health (Dublin, OH) and stored at room temperature. Deferoxamine, cefiderocol, and meropenem were reconstituted with 0.9% sodium chloride (normal saline [NS]). All compounds were subsequently diluted with NS to deliver the intended weight-based doses.

Animals. All animals were maintained and utilized in accordance with National Research Council recommendations, and all procedures were approved by the Hartford Hospital Institutional Animal Care and Use Committee (assurance number A3185-01). Specific-pathogen-free female ICR mice (CD-1; Charles River Laboratories, Inc., Wilmington, MA, USA), approximately 8 weeks old, were housed in HEPA-filtered cages in groups of 6 at controlled room temperature and were allowed to acclimate for 48 h before initiation of study procedures. Food and water were available *ad libitum*, and paper nesting material was provided for enrichment. A 12-h light/12-h dark cycle was maintained. Mice were monitored over the course of study for signs of morbidity; if loss of righting reflex was detected, mice were euthanized via CO_2 asphyxiation followed by cervical dislocation.

Iron overload and depletion models. All mice assigned to iron overload groups received a normal diet, while mice in the iron depletion groups received an iron-restricted diet (≤3 ppm) (LabDiet, St. Louis, MO). Groups of 12 mice received daily intraperitoneal (i.p.) injections of 100 mg/kg iron dextran (overload), a pharmaceutical source of iron, or 100 mg/kg deferoxamine (depletion), an iron chelator used clinically to treat iron overload, delivered in a volume of 0.2 ml for 14 days. Additional groups of 12 mice in the iron depletion model received 100 mg/kg deferoxamine i.p. daily for 30 days to study the effect of an extended treatment duration. Mice in control groups received 0.2 ml NS i.p. placebo injections on the same schedule as iron dextran or deferoxamine. The injection site was alternated daily between the left and right abdomen to reduce repeated trauma to the same location.

Mice in all groups (iron overload, iron depletion, and control) received treatments customarily used to prepare the neutropenic murine thigh infection model. Cyclophosphamide induces neutropenia, which permits the establishment of infection; doses of 150 mg/kg and 100 mg/kg i.p. were given 4 days and 1 day, respectively, before the completion of iron dextran or deferoxamine treatment. Uranyl nitrate causes acute tubular necrosis, which reduces renal clearance of renally cleared antibiotics, allowing their exposures to approximate human exposures; 5 mg/kg i.p. was given 3 days before the completion of iron dextran or deferoxamine treatment. Cyclophosphamide and uranyl nitrate doses were administered on the opposite side of the abdomen from the iron dextran, deferoxamine, or NS placebo injections administered on the same day.

On day 0, one untreated group of 12 control mice was harvested to serve as a baseline. After 14 days (iron dextran and deferoxamine) or 30 days (deferoxamine) of treatment, mice and matching control groups were harvested. Additional groups were harvested on day 17 (iron dextran and deferoxamine) and day 33 (deferoxamine), with matching controls to measure the degree to which tissue iron normalized after 3 days (i.e., duration of study for pharmacodynamic assessments) without treatment.

Plasma, liver, and spleen tissues were collected from all harvested animals. Blood was collected via cardiac puncture immediately following CO_2 asphyxiation and centrifuged for 10 min at 3,000 rpm to separate plasma, which was immediately frozen at −80°C until analysis. All liver lobes were harvested aseptically with the gallbladder removed. Spleens were harvested aseptically with perisplenic fat

removed. Organ tissues were weighed wet and then homogenized in 5 ml (liver) or 1 ml (spleen) of NS before being frozen at −80°C until analysis.

Pharmacokinetic studies. Cefiderocol and meropenem regimens were previously established in the neutropenic murine thigh infection model to replicate the human plasma pharmacokinetic profile after clinical doses of 2 g intravenously (i.v.) as a 3-h infusion every 8 h for each drug. The cefiderocol regimen consisted of doses of 15, 20, 25, 10, and 5 mg/kg administered at 0, 1, 2, 4, and 6 h, respectively, while the meropenem regimen consisted of doses of 65, 65, 45, and 45 mg/kg administered at 0, 1.25, 3.5, and 6 h, respectively, given every 8 h (1, 26).

Mice in the pharmacokinetic experiments received 14 days of iron overloading or 30 days of iron-depleting treatment as described above. Simultaneous experiments with age-matched control mice receiving no iron-altering treatments were conducted for each model. All mice received cyclophosphamide and uranyl nitrate as described above. On day 14 (overload) or day 30 (depletion), both thighs of all mice were inoculated intramuscularly with 0.1 ml of an ~10^7 CFU/ml bacterial suspension prepared from *Acinetobacter baumannii* 126 (internal designation; cefiderocol MIC, 8 mg/liter), which was previously used to confirm cefiderocol human-simulated regimens (1). The isolate was previously frozen at −80°C in skim milk and transferred twice sequentially, with 20 to 24 h of incubation time per transfer. Beginning 2 h after inoculation, groups of 6 mice in each model received the human-simulated regimens of cefiderocol or meropenem and were sacrificed at 4 different time points during the dosing regimens. Mice were euthanized by CO_2 exposure, followed by blood collection via intracardiac puncture and ultimately cervical dislocation. Blood samples were centrifuged at 3,000 rpm for 10 min to separate plasma, which was stored at −80°C until analyzed.

***Ex vivo* interaction study.** Mice were treated for 30 days with deferoxamine and then sacrificed 1, 3, or 7 days after the last dose. An equal number of untreated same-age controls were simultaneously sacrificed. Plasma from 4 mice was pooled and divided into 2 aliquots, to which 2 known concentrations of cefiderocol were added, and then frozen at −80°C until analysis. Experiments were performed in quadruplicate.

Sample preparation and analysis. Total iron content in all samples was assayed using inductively coupled plasma mass spectrometry, performed by PureHoney Technologies (Billerica, MA). This method liberates free iron from protein complexation and permits the assessment of total iron from all sources in the sample. Fifty-microliter aliquots of plasma samples were diluted to 4 ml in 2% nitric acid containing 200 ppb cobalt internal standard. Liver and spleen homogenates were vortexed, and then 25- and 50-μl aliquots of liver and spleen suspension, respectively, were diluted to 1 ml with 2% nitric acid, vortexed again, and centrifuged at 14,000 rpm for 15 min to remove any insoluble material, followed by dilution of 800 ml of supernatant to 4 ml with 2% nitric acid. A single-quadrupole mass spectrometer (Agilent 7700) was used with pulse detection for iron concentrations up to 62.5 ppb and analog detection for higher concentrations. Iron content in plasma is reported as a concentration (micrograms per deciliter). Iron content in solid tissue was normalized by organ weight and is reported as micrograms of iron per gram of wet tissue (micrograms/gram).

Cefiderocol concentrations in plasma were assayed at Shionogi (Osaka, Japan) using liquid chromatography-tandem mass spectrometry. Meropenem concentrations were assayed at the Center for Anti-Infective Research and Development using high-performance liquid chromatography-UV methodology with detection at 298 nm (30).

Statistical analysis. Measurements of iron content were assessed for normality using the Shapiro-Wilk test. Due to the nonnormal distribution of the measurements in some groups, median iron content per treatment group was compared to that of same-age controls using the nonparametric Mann-Whitney rank sum test. Median values with interquartile ranges (IQR) are reported. Differences in plasma concentrations of meropenem and cefiderocol between models were considered significantly different if there was no overlap in the 95% confidence intervals of the mean values.

ACKNOWLEDGMENTS

This study was funded by a grant from Shionogi & Co. Ltd., Osaka, Japan.

REFERENCES

1. Monogue ML, Tsuji M, Yamano Y, Echols R, Nicolau DP. 2017. Efficacy of humanized exposures of cefiderocol (S-649266) against a diverse population of Gram-negative bacteria in the murine thigh infection model. Antimicrob Agents Chemother 61:e01022-17. https://doi.org/10.1128/AAC.01022-17.
2. Ganz T, Nemeth E. 2012. Hepcidin and iron homeostasis. Biochim Biophys Acta 1823:1434–1443. https://doi.org/10.1016/j.bbamcr.2012.01.014.
3. Cassat JE, Skaar EP. 2013. Iron in infection and immunity. Cell Host Microbe 13:509–519. https://doi.org/10.1016/j.chom.2013.04.010.
4. Mislin GLA, Schalk IJ. 2014. Siderophore-dependent iron uptake systems as gates for antibiotic Trojan horse strategies against *Pseudomonas aeruginosa*. Metallomics 6:408–420. https://doi.org/10.1039/c3mt00359k.
5. Mochizuki H, Yamada H, Oikawa Y, Murakami K, Ishiguro J, Kosuzume H, Aizawa N, Mochida E. 1988. Bactericidal activity of M14659 enhanced in low-iron environments. Antimicrob Agents Chemother 32:1648–1654. https://doi.org/10.1128/aac.32.11.1648.
6. Ito A, Nishikawa T, Matsumoto S, Yoshizawa H, Sato T, Nakamura R, Tsuji M, Yamano Y. 2016. Siderophore cephalosporin cefiderocol utilizes ferric iron transporter systems for antibacterial activity against *Pseudomonas aeruginosa*. Antimicrob Agents Chemother 60:7396–7401. https://doi.org/10.1128/AAC.01405-16.
7. Fleming RE, Prem Ponka MD. 2012. Iron overload in human disease. N Engl J Med 366:348–359. https://doi.org/10.1056/NEJMra1004967.
8. Kowdley KV. 2016. Iron overload in patients with chronic liver disease. Gastroenterol Hepatol 12:695–698.
9. Brittenham GM. 2011. Iron-chelating therapy for transfusional iron overload. N Engl J Med 364:146–156. https://doi.org/10.1056/NEJMct1004810.
10. Lopez A, Cacoub P, Macdougall IC, Peyrin-Biroulet L. 2016. Iron deficiency anaemia. Lancet 387:907–916. https://doi.org/10.1016/S0140-6736(15)60865-0.
11. Gletsu-Miller N, Wright BN. 2013. Mineral malnutrition following bariatric surgery. Adv Nutr 4:506–517. https://doi.org/10.3945/an.113.004341.

12. Wessling-Resnick M. 2010. Iron homeostasis and the inflammatory response. Annu Rev Nutr 30:105–122. https://doi.org/10.1146/annurev.nutr.012809.104804.
13. Schalk IJ. 2018. Siderophore-antibiotic conjugates–exploiting iron uptake to deliver drugs into bacteria. Clin Microbiol Infect 24:801–802. https://doi.org/10.1016/j.cmi.2018.03.037.
14. Fleming RE, Feng Q, Britton RS. 2011. Knockout mouse models of iron homeostasis. Annu Rev Nutr 31:117–137. https://doi.org/10.1146/annurev-nutr-072610-145117.
15. Rivera S, Ganz T. 2009. Animal models of anemia of inflammation. Semin Hematol 46:351–357. https://doi.org/10.1053/j.seminhematol.2009.06.003.
16. Brittenham GM, Farrell DE, Harris JW, Feldman ES, Danish EH, Muir WA, Tripp JH, Bellon EM. 1982. Magnetic-susceptibility measurement of human iron stores. N Engl J Med 307:1671–1675. https://doi.org/10.1056/NEJM198212303072703.
17. Dongiovanni P, Valenti L, Fracanzani AL, Gatti S, Cairo G, Fargion S. 2008. Iron depletion by deferoxamine up-regulates glucose uptake and insulin signaling in hepatoma cells and in rat liver. Am J Pathol 172:738–747. https://doi.org/10.2353/ajpath.2008.070097.
18. Zhang W, Wei H, Frei B. 2010. The iron chelator, desferrioxamine, reduces inflammation and atherosclerotic lesion development in experimental mice. Exp Biol Med 235:633–641. https://doi.org/10.1258/ebm.2009.009229.
19. Hershko C, Peto TE. 1988. Deferoxamine inhibition of malaria is independent of host iron status. J Exp Med 168:375–387. https://doi.org/10.1084/jem.168.1.375.
20. Minqin R, Rajendran R, Pan N, Tan BKH, Ong WY, Watt F, Halliwell B. 2005. The iron chelator desferrioxamine inhibits atherosclerotic lesion development and decreases lesion iron concentrations in the cholesterol-fed rabbit. Free Radic Biol Med 38:1206–1211. https://doi.org/10.1016/j.freeradbiomed.2005.01.008.
21. Batts KP. 2007. Iron overload syndromes and the liver. Mod Pathol 20:S31–S39. https://doi.org/10.1038/modpathol.3800715.
22. Brissot P, Troadec MB, Loréal O, Brissot E. 2019. Pathophysiology and classification of iron overload diseases; update 2018. Transfus Clin Biol 26:80–88. https://doi.org/10.1016/j.tracli.2018.08.006.
23. Olivieri NF, Brittenham GM. 1997. Iron-chelating therapy and the treatment of thalassemia. Blood 89:739–761. https://doi.org/10.1182/blood.V89.3.739.
24. Cappellini MD, Cohen A, Piga A, Bejaoui M, Perrotta S, Agaoglu L, Aydinok Y, Kattamis A, Kilinc Y, Porter J, Capra M, Galanello R, Fattoum S, Drelichman G, Magnano C, Verissimo M, Athanassiou-Metaxa M, Giardina P, Kourakli-Symeonidis A, Janka-Schaub G, Coates T, Vermylen C, Olivieri N, Thuret I, Opitz H, Ressayre-Djaffer C, Marks P, Alberti D. 2006. A phase 3 study of deferasirox (ICL670), a once-daily oral iron chelator, in patients with β-thalassemia. Blood 107:3455–3462. https://doi.org/10.1182/blood-2005-08-3430.
25. Ward PP, Mendoza-Meneses M, Cunningham GA, Conneely OM. 2003. Iron status in mice carrying a targeted disruption of lactoferrin. Mol Cell Biol 23:178–185. https://doi.org/10.1128/mcb.23.1.178-185.2003.
26. Ghazi IM, Monogue ML, Tsuji M, Nicolau DP. 2018. Humanized exposures of cefiderocol, a siderophore cephalosporin, display sustained in vivo activity against siderophore-resistant *Pseudomonas aeruginosa*. Pharmacology 101:278–275. https://doi.org/10.1159/000487441.
27. Stainton SM, Monogue ML, Tsuji M, Yamano Y, Echols R, Nicolau DP. 2018. Efficacy of humanized cefiderocol exposures over 72 hours against a diverse group of Gram-negative isolates in the neutropenic murine thigh infection model. Antimicrob Agents Chemother 63:e01040-18. https://doi.org/10.1128/AAC.01040-18.
28. Tomaras AP, Crandon JL, McPherson CJ, Banevicius MA, Finegan SM, Irvine RL, Brown MF, O'Donnell JP, Nicolau DP. 2013. Adaptation-based resistance to siderophore-conjugated antibacterial agents by *Pseudomonas aeruginosa*. Antimicrob Agents Chemother 57:4197–4207. https://doi.org/10.1128/AAC.00629-13.
29. Kim A, Kutschke A, Ehmann DE, Patey SA, Crandon JL, Gorseth E, Miller AA, McLaughlin RE, Blinn CM, Chen A, Nayar AS, Dangel B, Tsai AS, Rooney MT, Murphy-Benenato KE, Eakin AE, Nicolau DP. 2015. Pharmacodynamic profiling of a siderophore-conjugated monocarbam in *Pseudomonas aeruginosa*: assessing the risk for resistance and attenuated efficacy. Antimicrob Agents Chemother 59:7743–7752. https://doi.org/10.1128/AAC.00831-15.
30. Elkhaïli H, Linger L, Monteil H, Jehl F. 1997. High-performance liquid chromatographic assay for cefepime in serum. J Chromatogr B Biomed Sci Appl 690:181–188. https://doi.org/10.1016/S0378-4347(96)00406-9.